



OPEN ACCESS

EDITED BY

Sheng-Hong Li,
Chinese Academy of Sciences (CAS), China

REVIEWED BY

Ping Li,
South China Agricultural University, China
Krishna Ray,
West Bengal State University, India

*CORRESPONDENCE

Yao Ma

✉ mayao@zzu.edu.cn

Yueteng Zhang

✉ yuetengzhang@zzu.edu.cn

Kangdong Liu

✉ kdliu@zzu.edu.cn

RECEIVED 22 May 2024

ACCEPTED 10 September 2024

PUBLISHED 26 September 2024

CITATION

Xie L, Chen Q, Cheng N, Zhang Y, Ma Y, Zhang Y and Liu K (2024) Integrated metabolomic and transcriptomic analyses of *Dendrobium chrysotoxum* and *D. thyrsiflorum* reveal the biosynthetic pathway from gigantol to erianin. *Front. Plant Sci.* 15:1436560. doi: 10.3389/fpls.2024.1436560

COPYRIGHT

© 2024 Xie, Chen, Cheng, Zhang, Ma, Zhang and Liu. This is an open-access article distributed under the terms of the [Creative Commons Attribution License \(CC BY\)](https://creativecommons.org/licenses/by/4.0/). The use, distribution or reproduction in other forums is permitted, provided the original author(s) and the copyright owner(s) are credited and that the original publication in this journal is cited, in accordance with accepted academic practice. No use, distribution or reproduction is permitted which does not comply with these terms.

Integrated metabolomic and transcriptomic analyses of *Dendrobium chrysotoxum* and *D. thyrsiflorum* reveal the biosynthetic pathway from gigantol to erianin

Lihang Xie¹, Qiuying Chen², Najing Cheng¹, Yue Zhang¹, Yao Ma^{2*}, Yueteng Zhang^{1*} and Kangdong Liu^{3*}

¹Tianjian Laboratory of Advanced Biomedical Sciences, Academy of Medical Sciences, Zhengzhou University, Zhengzhou, Henan, China, ²School of Agricultural Sciences, Zhengzhou University, Zhengzhou, China, ³Department of Pathophysiology, Basic Medicine Research Center, School of Basic Medical Sciences, Zhengzhou University, Zhengzhou, China

Erianin is one of the most representative bibenzyls with significant inhibitory activity against a wide range of tumor cells. However, the low erianin level in natural materials has severely inhibited its further development in health care. Our aim was to uncover the erianin biosynthetic pathway to lay the foundation for promoting its production. Firstly, we screened and obtained two *Dendrobium* species (*Dendrobium thyrsiflorum* stems with lower erianin content and *D. chrysotoxum* stems with higher erianin content), belonging to the same *Dendrobium* section (Chrysotoxae). A systematic analysis of bibenzyl structure and content in two stems revealed that gigantol might be an erianin biosynthetic intermediate, which was verified by introducing deuterium-labeled gigantol. Chemical structure analyses indicated that gigantol was modified by two kinds of enzymes (hydroxylases and O-methyltransferases), leading to erianin synthesis. Up-regulated hydroxylases and O-methyltransferases (OMTs) were screened out and were performed by molecular docking simulation experiments. We propose a rational biosynthetic pathway from gigantol to erianin, as well as relevant enzymes involved in the process. Our findings should significantly contribute to comprehensive resolution of the erianin biosynthetic pathway, promote its large-scale industrial production as well as contribute to biosynthesis studies of other bibenzyls.

KEYWORDS

dendrobium, erianin, biosynthetic pathway, metabolomics, transcriptomics

Introduction

Erianin (2-methoxy-5-[2-(3,4,5-trimethoxy-phenyl)-ethyl]-phenol), the representative bibenzyl compounds (Su et al., 2017), has been used in health care for the biological activities such as anti-inflammatory (Zhang et al., 2019a), anti-oxidant (Chen et al., 2019) and anti-bacterial (Yuan et al., 2018). Notably, it has been demonstrated to possess significant anti-tumor effects on various cancer cell lines *in vitro* and *in vivo* (Qiao et al., 2022). Erianin can inhibit the proliferation of different tumor cells through various mechanisms, inducing cell differentiation, apoptosis, or autophagy, arresting cell cycle, inhibiting tumor angiogenesis, and affecting cell migration and invasion (Zhang et al., 2019b). Overall, erianin is an active anti-cancer component with great potential. Erianin is mainly found in *Dendrobium chrysotoxum* (DC) stems, with only 0.12% of the yield, it can barely meet the needs of anti-cancer drug development and market needs (Luo et al., 2019; Qiao et al., 2022).

Artificially synthesized erianin can be a suitable strategy to compensate for its shortage of natural resources. Although the chemical synthesis of erianin has been previously reported, it has not been widely adopted because of high cost and the inevitable production of polluting by-products during its synthesis (Zou et al., 2008). Recent biosynthetic technological developments offer alternative opportunities for low cost erianin production. Naturally, the first step of synthetic biology is to elucidate biosynthetic pathway of target component. However, the biosynthetic pathway of erianin is not entirely clear (Adejobi et al., 2021).

Recently, the physiological and molecular mechanisms underlying bibenzyl compound biosynthesis were investigated using transcriptomic analyses of MethylJasmonate (MeJA)-treated *D. officinale* roots (Adejobi et al., 2021). Two candidate cytochrome P450 genes and nine other enzymatic genes might be functionally involved in bibenzyl biosynthesis. Generally, the first step in bibenzyl compound synthesis is the production of cinnamic acid catalyzed by phenylalanine ammonia-lyase (PAL) with L-Phenylalanine as substrate. Then, cinnamate 4-hydroxylase (C4H) catalyzes the conversion of cinnamic acid into two isomers (*m*-coumaric acid and *p*-coumaric acid). Finally, 3,3'-trihydrobibenzyl is produced with subsequent catalyzation of CYP450, 4-coumarate-CoA ligase (4CL), and bibenzyl synthase (BBS), employing *m*-coumaric acid as substrate. However, the biosynthetic pathway between 3,3'-trihydrobibenzyl and erianin is still unclear.

D. thyrsiflorum (DT), belonging to the same *Dendrobium* section (Chrysotoxae) as DC, was found to contain smaller amounts of erianin (Luo et al., 2019). In this study, a combined metabolome and transcriptome approach was employed to investigate erianin biosynthesis differences between DT and DC, shedding light on how erianin is synthesized in *Dendrobium* plants. Gigantol was found to be a possible intermediate in the biosynthesis pathway of erianin, and the structural genes related to the synthesis of erianin were initially identified. Our studies are of great significance for comprehensively elucidating erianin biosynthetic pathway and would provide a guidance for future synthetic biology strategies.

Materials and methods

Plant materials

Two-year-old DC and DT stems were collected from the same plantation at Ning'er Hani Yi Autonomous County, Pu'er City, Yunnan, China (101°03'8.79"N, 23°03'16.52"E). Each stem was divided into two parts along growth direction. One-half of the stem was used for metabolomic analysis, and the other half was used for transcriptomic analysis. Three biological replicates were performed for each sample. All samples were immediately frozen in liquid nitrogen and kept at -80° for further use.

Widely targeted metabolome analysis

Widely targeted metabolome analysis was performed by Metware Biotechnology Co., Ltd. (Wuhan, China) following their standard procedures. Briefly, 100 mg of lyophilized powder was dissolved with 1.2 mL 70% methanol solution, vortexed 30 seconds every 30 minutes for 6 times in total, and then placed in a refrigerator at 4°C overnight. After centrifuged at 12000 rpm for 10 min, the extracts were filtrated through a 0.22 μm polytetrafluoroethylene (PTFE) membrane (MF, Millipore) before UPLC-MS/MS analysis.

The sample extracts were analyzed using an UPLC-ESI-MS/MS system (UPLC, SHIMADZU Nexera X2; MS, Applied Biosystems 4500 Q TRAP). The analytical conditions were as follows, UPLC: column, Agilent SB-C18 (1.8 μm, 2.1 mm x 100 mm); The mobile phase was consisted of solvent A, pure water with 0.1% formic acid, and solvent B, acetonitrile with 0.1% formic acid. Sample measurements were performed with a gradient program that employed the starting conditions of 95% A, 5% B. Within 9 min, a linear gradient to 5% A, 95% B was programmed, and a composition of 5% A, 95% B was kept for 1 min. Subsequently, a composition of 95% A, 5.0% B was adjusted within 1.1 min and kept for 2.9 min. The flow velocity was set as 0.35 mL per minute; The column oven was set to 40°C; The injection volume was 4 μL. The effluent was alternatively connected to an ESI-triple quadrupole-linear ion trap (QTRAP)-MS.

Metabolite identification and quantification were performed using the self-built MetWare database and other public databases. The scheduled multiple reaction monitoring (MRM) method was previously described by Chen et al (Chen et al., 2013). All the bibenzyl were further screened out based on the chemical structures.

Introduction of label and identification

The introduction of ²H (D) label was performed by adding D-gigantol dissolved with DMSO, which was chemically synthesized in our laboratory and verified by NMR, at a final concentration of 50 mM to the buffer solution (10 mM MES + KOH, pH 6.5). The stems pieces of DC from six independent plants were mixed and incubated for 5 h in buffer solution under vacuum. At the end of the incubation, stems were snap-frozen in liquid nitrogen. They were

subsequently extracted using 100% methanol and filtered through a 0.22 μm filter membrane.

Chromatographic analysis was carried out using a Waters Acquity UPLC system (Waters Corp., Milford, MA, USA) with a waters BEH C18 column (1.7 μm , 2.1 \times 50 mm) at a temperature of 40°C. Gradient elution with 0.1% of formic acid aqueous solution (A) and acetonitrile solution (B) was employed at a flow rate of 0.4 mL/min, with the following gradient program: 0–1 min 5% B, 1–7 min 5%–98% B, 7–10 min 98% B. The injection volume was 1 μL .

Mass spectrometric detection was performed on Waters Xevo G2-XS QTOF mass spectrometer (Waters Corp., Milford, MA, USA) equipped with an ESI source. Source conditions included a source temperature and desolvation gas temperature of 110 and 400°C, respectively, cone gas flow and desolvation gas (N_2) flow of 100 and 800 L/h, respectively, and sampling cone voltage of 40 V, with a capillary voltage of 2.5 kV for positive ion mode. TOF parameters included a full scan analysis with a mass range from 50 to 1200 Da and collision energy set as 6.0 eV for low-energy scan and 20–30 eV for high-energy scan.

RNA extraction, illumine sequencing, and transcriptome data analysis

Six total RNA samples (two different groups with three replicates) were isolated using the RNAPrep Pure Plant Plus Kit (#DP441; Tiangen, <http://www.tiangen.com>) according to the manufacturer's instructions, and a 1% agarose gel and a Nano spectrophotometer (IMPLEN, CA, USA) were used to test the concentration of the total RNA. The cDNA library construction and RNA-seq were performed by Metware Biotechnology Co., Ltd. (Wuhan, China). A total of 1 μg RNA per sample was used to generate a cDNA library using the NEBNext[®] UltraTM RNA Library Prep Kit (NEB, USA) according to the manufacturer's instructions. The libraries were then sequenced on an illumina Hiseq platform. The original data were filtered to remove reads with adapters using fastp v 0.19.3. Then, the clean reads were mapped to the *D. catenatum* reference genome (https://www.ncbi.nlm.nih.gov/datasets/genome/GCF_001605985.2/) using the default parameters of Hisat2 software (Li et al., 2020). Fragments per kilobase of transcript per million mapped reads (FPKM) were used for transcription or quantification of gene expression levels. An absolute log₂ (fold change) ≥ 1 and false discovery rate (FDR) < 0.05 were used as thresholds for the identification of differentially expressed genes (DEGs) using DESeq2 software. Gene Ontology (GO) enrichment analysis was performed using the GOSec R package (corrected *p*-value < 0.05). Pathway analysis was performed to elucidate the significant pathways of DEGs using Kyoto Encyclopedia of Gene and Genomes (KEGG) (<http://www.genome.jp/kegg>).

Phylogenetic and molecular evolutionary analyses

The Hydroxylases and OMTs from different species were selected from the National Center for Biotechnology Information

(NCBI) database (<https://www.ncbi.nlm.nih.gov/>) for the construction of a maximum likelihood phylogenetic tree. Multiple sequence alignment was performed with DNAMAN version 5.2.2. Molecular Evolutionary Genetics Analysis (MEGA) version X was applied for the phylogenetic and molecular evolutionary analysis. The phylogenetic tree was annotated using Evolview v3 (Zhang et al., 2012).

Homologous modelling and molecular docking

The homology structural models of hydroxylases and OMTs were built by SWISS-MODEL modelling server. The model quality was validated via ProSA-web (Wiederstein and Sippl, 2007), QMEAN version 4.3.0 (Benkert et al., 2008) and SAVES v6.0 (<https://saves.mbi.ucla.edu/>). The 3D structures of gigantol (PubChem CID: 3085362) and Compound 1 (PubChem CID: 153349) were obtained in structural data format (SDF) from PubChem database (<https://pubchem.ncbi.nlm.nih.gov/>), while that of Compound 2 was prepared using Chem3D by CambridgeSoft. The differentially expressed Hydroxylases and OMTs from DC were subjected to an In-silico molecular docking study with the help of AutoDockTool-4.2 (Morris et al., 2009), in which the grid box was set to X = 108.15, Y = 108.15 and Z = 108.15 with spacing = 0.858 Å for Compound 1, X = 92.05, Y = 92.05 and Z = 92.05 with spacing = 0.731 Å for gigantol (3) and Compound 2, covering all the reported active residues. These tools also aid to forecast the binding stability between the two molecules by means of the scoring function. Individually the protein-ligand was observed through the Pymol (Yuan et al., 2017) and Discovery Studio 2019 Client (An et al., 2020).

Statistical analysis

The experimental data, consisting of three independent biological replicates, were subjected to statistical analysis using SPSS version 21.0. One-way analysis of variance was followed by Duncan's tests, with a significance level set at *p* < 0.05 . A heatmap of erianin biosynthesis-related genes was constructed based on transcriptome data using TBtools. The evolution tree of differentially expressed hydroxylases and OMTs was performed by OmicShare.

Results and discussion

Selection of materials for investigating erianin biosynthetic pathway

Only a few wild *Dendrobium* species were found to contain erianin, among which DC had the highest erianin content, accounting for about 0.12% of the mass fraction (Luo et al., 2019). Although DT and DC belong to the same *Dendrobium* section, the content of erianin in DT stem was only 0.008% (Figure 1A). Moreover, comparative metabolomic analysis

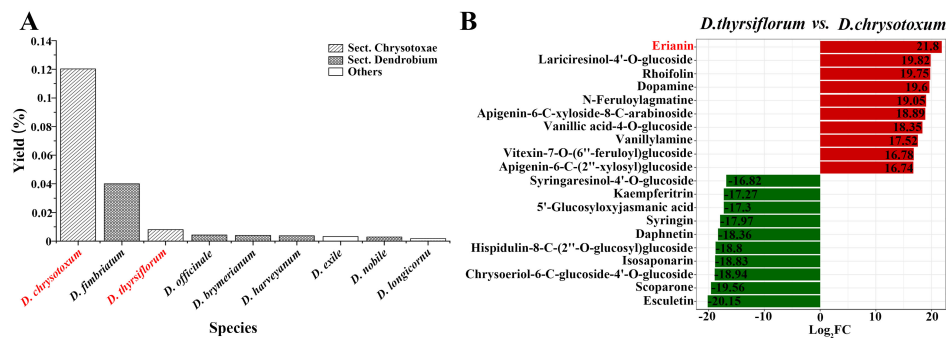


FIGURE 1 Erianin content in different wild *Dendrobium* species (A); Top 10 differential secondary metabolites in DT and DC stems (B).

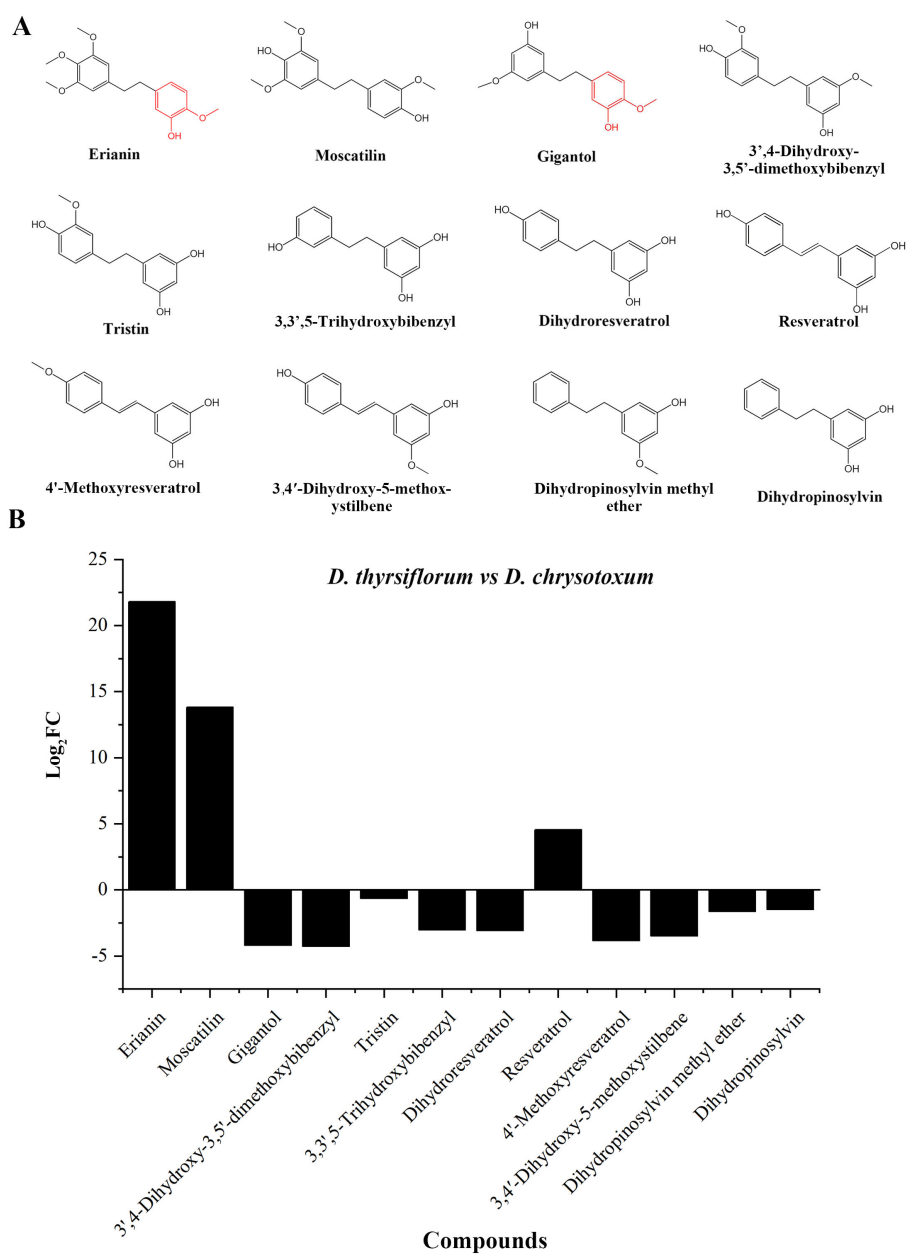


FIGURE 2 Bibenzylic compounds identified in the metabolome. (A) Structure of identified bibenzylic compounds; (B) Difference in the relative content of identified compounds in the stems of DT and DC.

showed that erianin was the secondary metabolite that differed the most in content between the two *Dendrobium* species (Figure 1B, Supplementary Table S1). Therefore, DC and DT are good research materials for exploring the biosynthetic pathway of erianin.

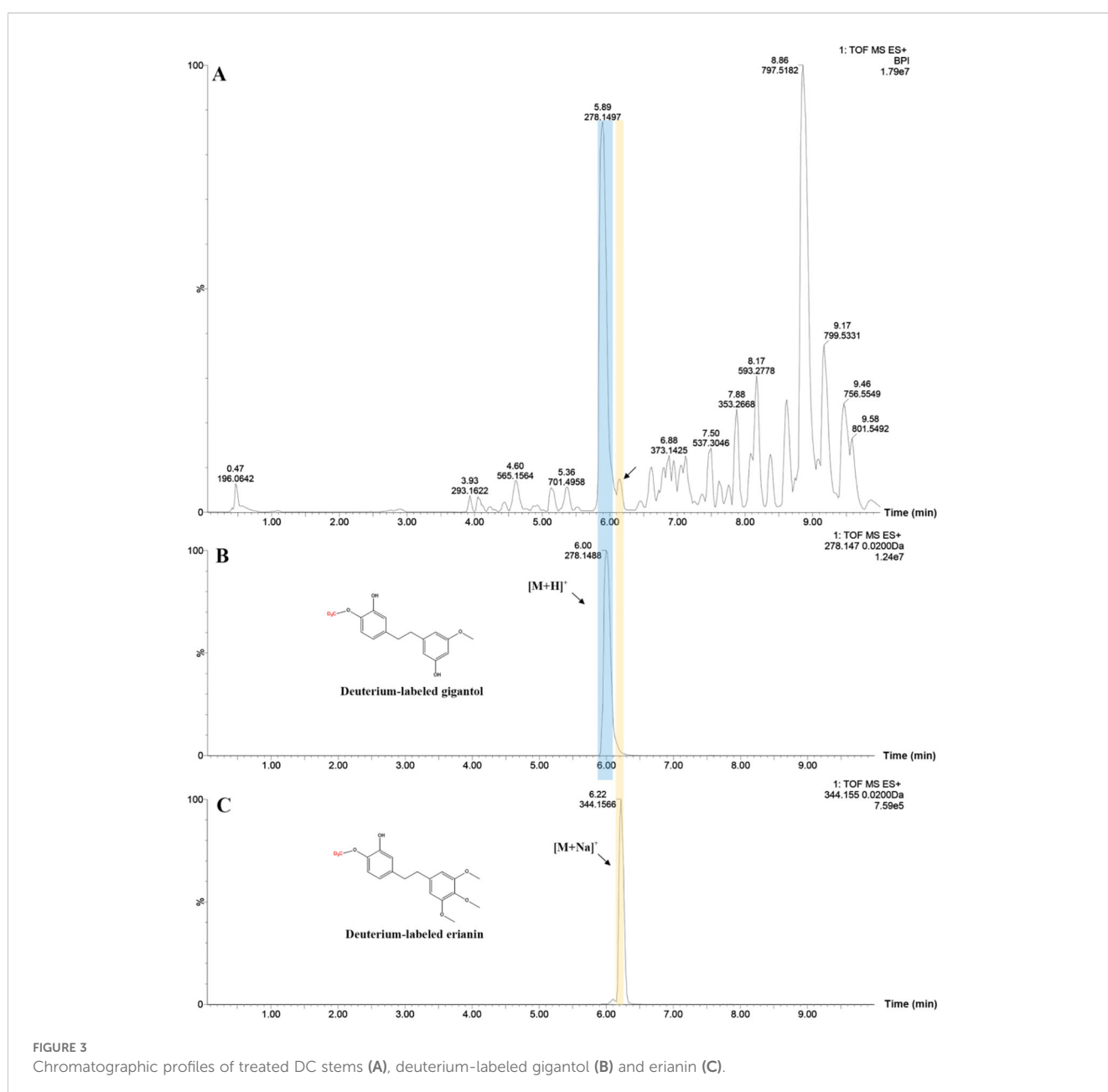
Gigantol is a possible intermediate in erianin biosynthesis pathway

To discover possible intermediates in the erianin synthesis pathway, the substances detected by the metabolome were further screened and analyzed. A total of 11 bibenzyl compounds structurally similar to erianin were discovered (Figure 2). Based on chemical structure analysis, gigantol and erianin were the most structurally similar, especially in one of the benzene rings, where

both were methoxy in the para position and hydroxyl in the interposition. Moreover, the content of erianin was significantly higher than that of gigantol in DC, when compared to DT. Similar results also have been reported previously (Duo et al., 2018). Therefore, gigantol is more likely to be consumed and further modified to synthesize erianin, resulting in low content of gigantol in DC stems.

Validation of gigantol as a potential intermediate for erianin biosynthesis

To determine if gigantol could act as an intermediate substance for erianin biosynthesis, the deuterium-labeled gigantol was employed. By vacuuming, deuterium-labeled



gigantol was pumped into DC stems, which were previously cut into small pieces. LC-MS results showed that deuterium-labeled gigantol and erianin were detected in treated DC stems extracts (Figure 3, Supplementary Figure S1). Indeed, isotopic tracers are used to both trace metabolic pathways and quantify fluxes through these pathways (Schwender, 2008; Chassy et al., 2014). But, the use of deuterium feeding in the way is quite rare in the studies on the biosynthetic pathway of plant secondary metabolites, except the

study using mechanism-directed deuterium labeling for the tracing of benzylisoquinoline alkaloid biosynthesis in *Papaver somniferum* (Vavricka et al., 2022). The deuterium-labeled gigantol and erianin at the same site were designed and produced by our laboratories based on their chemical structures, which provided an excellent tool for the validation of previous inferences. Since deuterium is not a common element in nature, the detection of deuterium-labeled erianin in DC stems after being

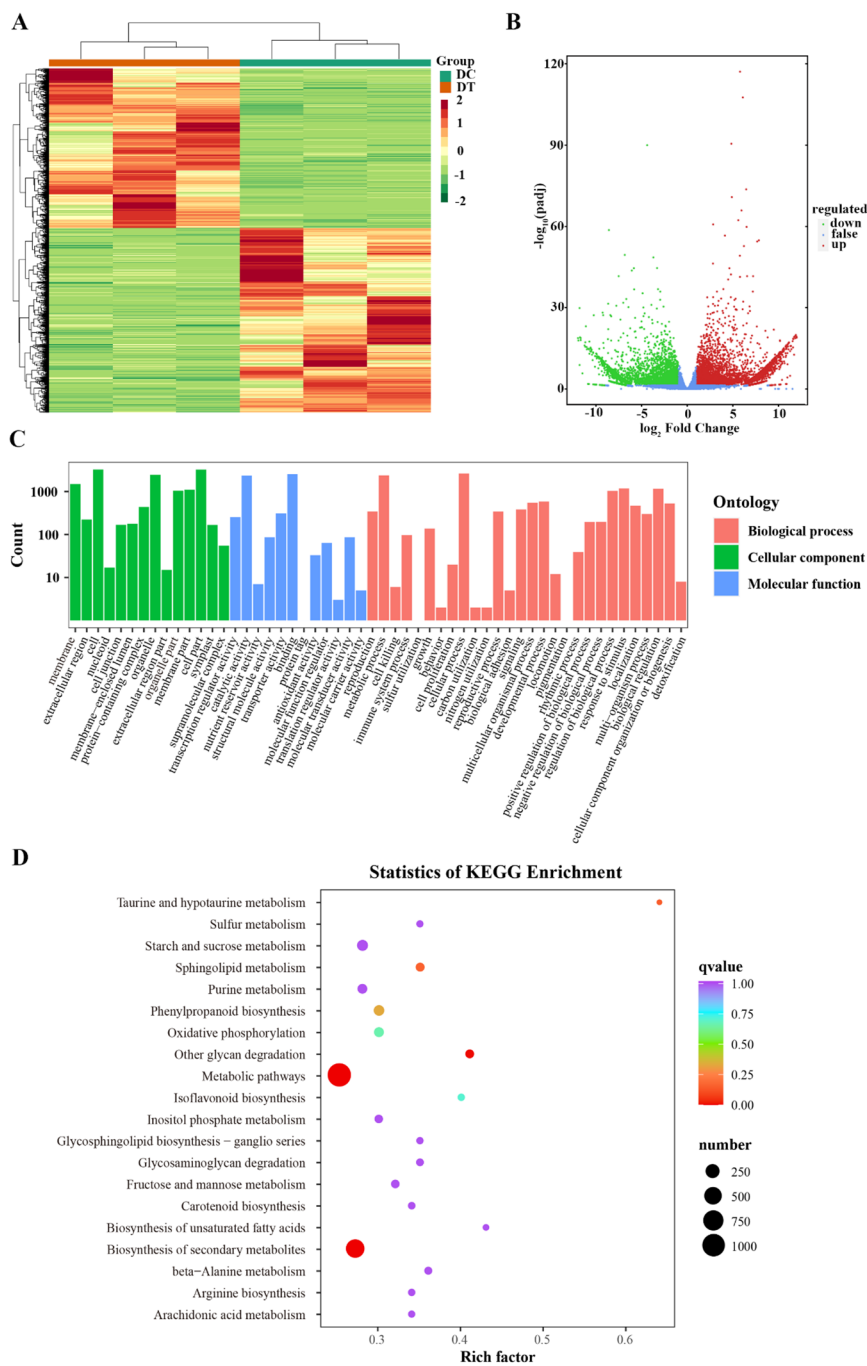


FIGURE 4 Analysis of differentially expressed genes (DEGs) between DC and DT. (A) Heat map of DEGs based on hierarchical clustering analysis; (B) Volcano plots of DEGs. The red dots represent the significantly upregulated genes, and the green dots represent the significantly downregulated genes; (C) GO enrichment analysis of DEGs in the three functional groups; (D) Scatter plots of top 20 KEGG pathways with the most significant enrichment.

fed with deuterium-labeled gigantol further suggests that gigantol is likely to be one of the potential intermediates for erianin biosynthesis. In addition to this, trace amounts of erianin were detected possibly due to isotope discrimination, which incorporates D relative to the equivalent H during reactions, and the inactivation of enzymes in stems after isolation (Werner and Schmidt, 2002).

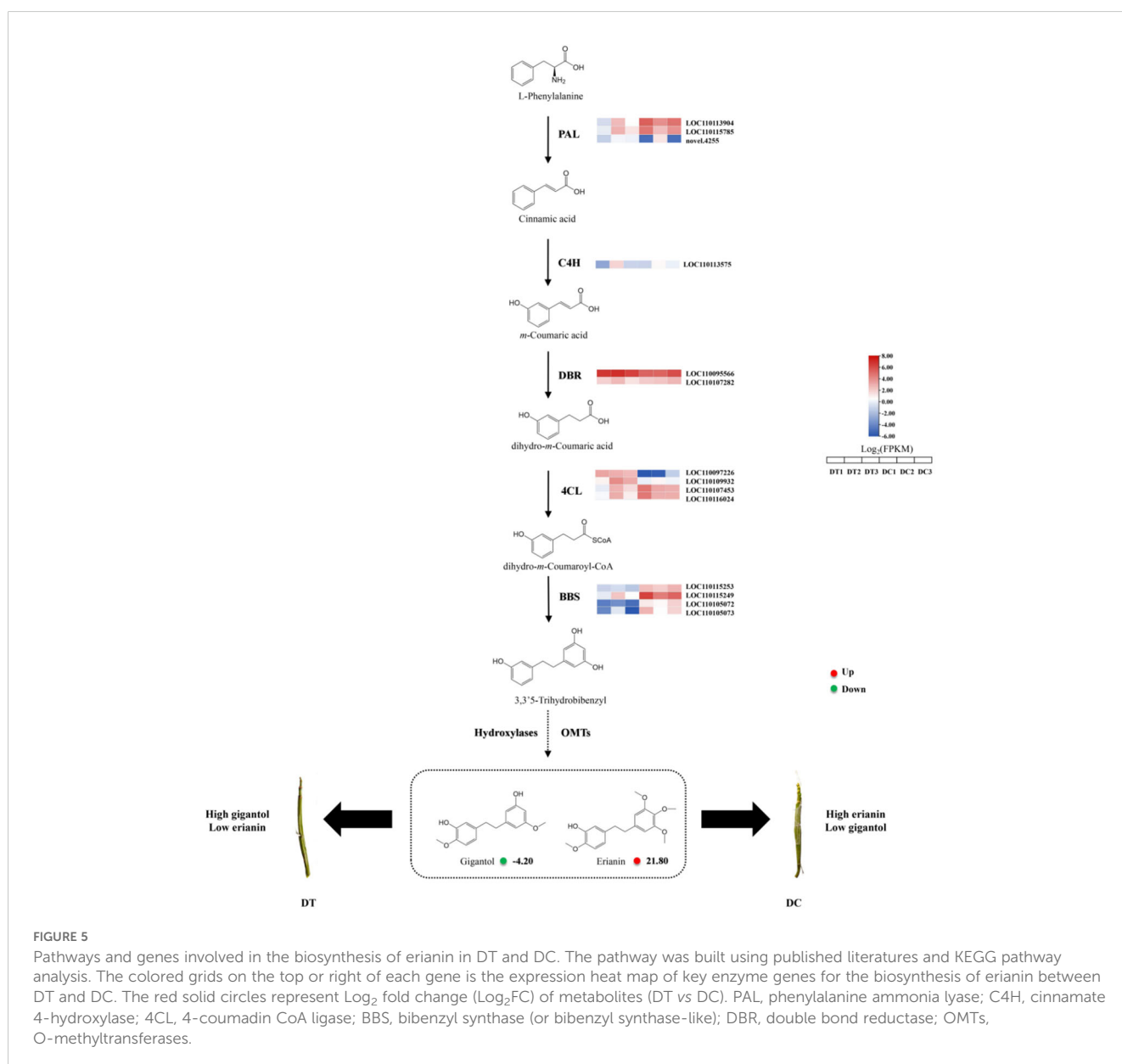
Overview of the transcriptome sequencing

In order to investigate the molecular mechanism of erianin biosynthesis, RNA-Seq was employed for transcriptome analysis. Stems of DT and DC were collected and used to construct six sequencing libraries, namely DC1, DC2, DC3, DT1, DT2, and DT3. In total, 40.14 Gb of raw data with 94.04% of average clean Q30 were obtained from the six libraries (Supplementary Table S2). Of

all clean reads, 72.07 to 80.80% were mapped to the *D. catenatum* reference genome. A total of 29,028 expressed genes in DC stems and 27,842 expressed genes in DT stems were detected. The correlation analysis and principal component analysis (PCA) of samples showed high reproducibility between the biological replicates (Supplementary Figure S2).

DEG identification and enrichment analysis

A total of 7,992 DEGs were identified, including 3,706 downregulated, and 4,286 upregulated genes, in DC relative to DT comparisons with fold change ≥ 2 and FDR (False Discovery Rate) < 0.05 as filter criteria (Figures 4A, B, Supplementary Table S3). Enrichment analysis of GO functions showed that all DEGs could be divided into three functional groups: biological processes, cellular components, and molecular functions (Figure 4C). As



expected, many DEGs were associated with metabolic and cellular processes in the “biological process” category. In the cellular component class, numerous genes were annotated to participate in “cell part”, “cell”, and “organelle” processes. In the molecular function category, the most DEGs were enriched in the ‘binding’ and ‘catalytic activity’ subcategories. The KEGG pathway enrichment analysis revealed that DEGs were mainly enriched in ‘metabolic pathway (ko01100)’ and ‘biosynthesis of secondary metabolites (ko01110)’ (Figure 4D).

The differences in erianin biosynthesis pathway between DT and DC

To understand the biosynthesis mechanism of erianin, the integrative metabolomic and transcriptomic analysis between DT and DC was carried out (Figure 5). The expression of four BBS genes (LOC110115253, LOC110115249, LOC110105072, and LOC110105073) were significantly higher in DC than that in DT stems. The high expression of BBS genes leads to sufficient accumulation of intermediates for the synthesis of erianin in DC stems. In orchid species, BBS was first isolated and purified from

Bletilla striata, and bibenzyls were formed in large amounts with the activity of BBS in orchid rhizomes (Reinecke and Kindl, 1994). Therefore, BBS genes played a key role in bibenzyl biosynthesis in Orchid species. Similar conclusions also were found in *D. sinense* BBS. *DsBBS* genes were characterized by the combination of genes expressions and bibenzyl contents, and the key *DsBBS* gene was identified to specifically catalyze the cyclization and aromatization of 4-coumaryl-CoA and malonyl-CoA to generate resveratrol (Chen et al., 2022). Moreover, the content of resveratrol in DC stems was significantly higher than its content in DT, which was consistent with the results of the transcriptome (Supplementary Table S1). Conversely, resveratrol is catalyzed to produce more 4'-Methoxyresveratrol and 3,4'-Dihydroxy-5-methoxystilbene by OMTs in DT stems. Although the amount of dihydroresveratrol in DC stems was slightly less than in DT, the difference was statistically insignificant. Furthermore, dihydroresveratrol is catalyzed by the combined action of OMTs and hydroxylases to produce gigantol and erianin. Similar results were also found in *D. officinale*, where 3,3',5'-trihydrobibenzyl, the isomer of dihydroresveratrol, is regarded as the synthetic intermediates of gigantol and erianin with the catalyzation of OMTs and hydroxylases (Adejobi et al., 2021). Therefore, differences in the expression of OMT and hydroxylases

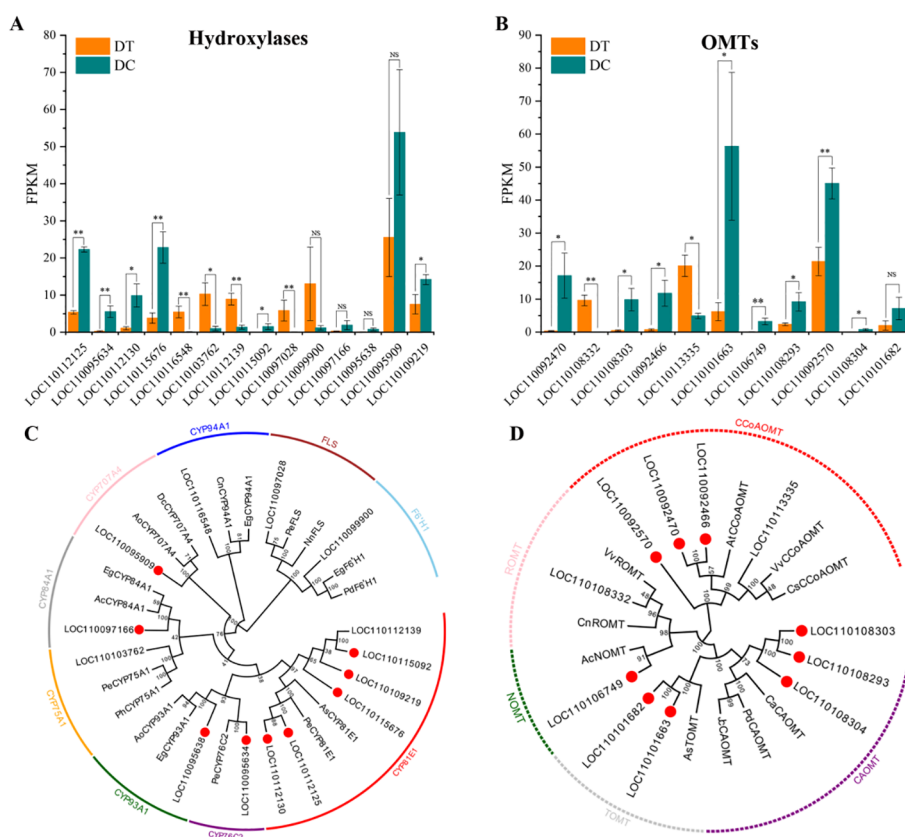


FIGURE 6 The comprehensive analysis of differentially expressed hydroxylases and OMTs. All the differentially expressed hydroxylases (A), and OMTs (B) between DT and DC. *, 0.01 < P ≤ 0.05; **, P ≤ 0.01; NS, not significant. Phylogenetic analysis of hydroxylases (C) and OMTs (D). Numbers on branches indicate the bootstrap percentage values calculated from 1000 bootstrap replicates. Genes marked with red circles show that it was significantly up-regulated in DC stems (Log2FC>1, p<0.05). Sequence accession numbers are given in Supplementary Table S4.

are likely to be the main factors responsible for differences in the contents of gigantol and erianin in DT and DC.

Candidate hydroxylases and OMTs related to erianin biosynthesis

To further identify key genes that may play an important role in the biosynthetic pathway of erianin, the differentially expressed hydroxylases and OMTs were analyzed (Figures 6A, B). A total of 14 hydroxylases and 11 OMTs with differential expression were identified based on the comparative transcriptome analysis. Among them, the expression of 9 hydroxylases and 9 OMTs were significantly upregulated and positively correlated with the accumulation of erianin in DC stems.

A neighbor-joining phylogenetic analysis was conducted using the selected hydroxylases and OMTs in this study, and those previously reported in other plants by MEGA X. Hydroxylases were divided into nine groups with the most belonging to cytochrome P450 (CYPs) family (Figure 6C). CYPs are monooxygenases encoded by a family of super genes, which are involved in a variety of plant metabolic reactions playing important roles in plant growth and stress response regulation mechanisms (Cui et al., 2020). Five upregulated hydroxylases in DC stems belong to the CYP81E1 group. CYP81E1 proteins, also known as isoflavone 2'-hydroxylase-like, share a high sequence homology with *Apostasia shenzhenica* and *Phalaenopsis equestris*, which have a close divergence time with *D. catenatum* (Zhang et al., 2020). Isoflavone 2'-hydroxylase also has been identified in soybean (Overkamp et al., 2000), chickpea, and alfalfa (Liu et al., 2003), and

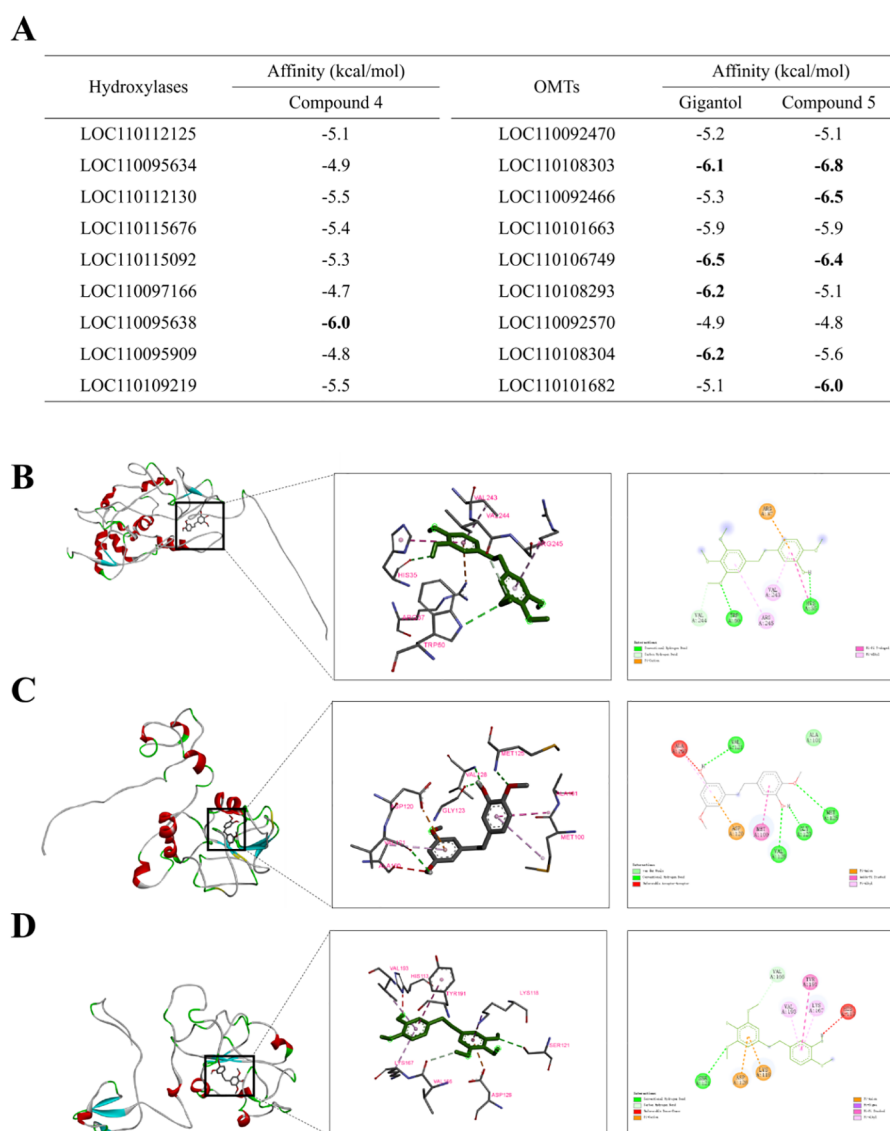


FIGURE 7

Results of molecular docking between substrates (compound 1, gigantol and compound 2) and key enzymes. (A) binding energy between the individual compounds and target proteins predicted by AutoDock Vina. The global diagrams and the details and the 2D diagrams of the docking between compound 1 and LOC110095638 (B), gigantol and LOC110106749 (C), compound 2 and LOC110108303 (D).

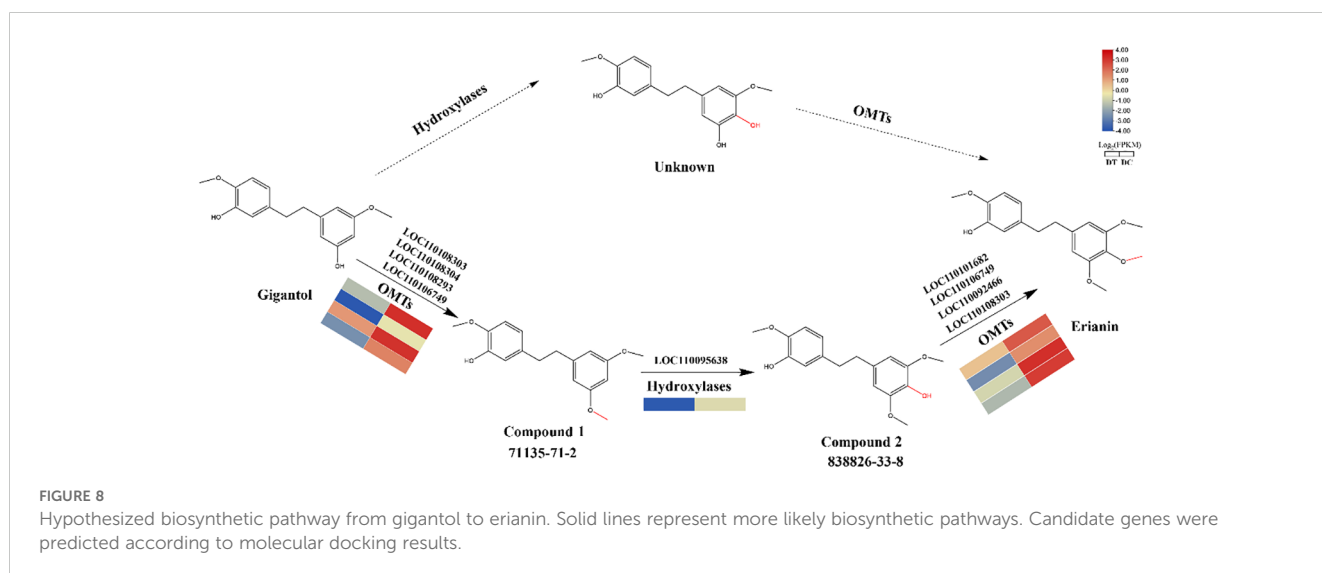
recombinant CYP81E1 were reported to catalyze 2'-hydroxylation of formononetin (7-hydroxy, 4'-methoxyisoflavone) and the 2'- and 3'-hydroxylation of daidzein (7,4'-dihydroxyisoflavone) *in vitro* in yeast microsomes (Akashi et al., 1998).

According to the phylogenetic analysis, differentially expressed OMTs were divided into 5 groups, including caffeoyl-CoA O-methyltransferase (CCoAOMT), trans-resveratrol di-O-methyltransferase (ROMT), (RS)-nordoclaurine 6-O-methyltransferase (NOMT), tricetin 3',4',5'-O-trimethyltransferase (TOMT), and caffeic acid 3-O-methyltransferase (CAOMT) (Figure 6D). The up-regulated OMTs mainly belong to CCoAOMT and CAOMT groups. Based on protein's size, substrate preference, and Mg²⁺ dependence, plant OMTs could be categorized into two major classes (Noel et al., 2003; Lam et al., 2007). Class I OMTs, also called CCoAOMTs, vary from 231 to 248 amino acids and require Mg²⁺ to perform its methylation. Unlike Class I OMTs, Class II OMTs are larger in length (344-383 aa) and act on a diverse group of compounds, such as CAOMT, ROMT (resveratrol O-methyltransferase), and others. Both CCoAOMT and CAOMT belong to the family of S-adenosyl-L-methionine (SAM) dependent O-methyltransferase and catalyze the conversion of caffeoyl-CoA to feruloyl-CoA, and caffeic acid into ferulic acid in lignin biosynthesis, respectively (Zhang et al., 2015; Narnoliya et al., 2021). CCoAOMTs and CAOMTs have been identified in a variety of vascular plants, including poplar (Zhong et al., 2000), alfalfa (*Medicago sativa*) (Marita et al., 2003), tobacco (*Nicotiana tabacum*) (Zhong et al., 1998), Arabidopsis (*A. thaliana*) (Do et al., 2007), and maize (*Zea mays*) (Yang et al., 2017). Lignin is the main component of *Dendrobium* stems (Yang and Liu, 2014; Mantovani et al., 2018), so the identification of CCoAOMTs and CAOMTs in DT and DC is reasonable. Moreover, CCoAOMTs and CAOMTs were found to be possibly redundant with respect to the methylation (Inoue et al., 1998). Therefore, the discovery of up-regulated CCoAOMTs and CAOMTs in DC stems also suggests that the biosynthesis of erianin could potentially occur via two parallel pathways.

Molecular docking analysis and a proposed biosynthetic pathway from gigantol to erianin

Based on the above findings, a biosynthetic pathway from gigantol to erianin was proposed. Theoretically, the biosynthesis of erianin from gigantol normally required the modifications by hydroxylases and OMTs. However, it was found that gigantol would generate unknown compounds, whose chemical structure was not recorded in the databases (SciFinder and PubChem), when not first modified by hydroxylases (Bari et al., 2021). In contrast, gigantol is more likely to be first modified by OMTs to produce compound 1 (5-(2-(3,5-dimethoxyphenyl)ethyl)-2-methoxy-, 71135-71-2), then by hydroxylases to produce compound 2 (4-[2-(3-hydroxy-4-methoxyphenyl)ethyl]-2,6-dimethoxy-, 833826-33-8), which is an isomer of moscatilin (a common secondary metabolite in DC stems) (Xia et al., 2023), and finally by OMTs to produce erianin. Therefore, the proposed biosynthetic pathway of gigantol firstly modified by OMTs is relatively reasonable.

To further refine the proposed biosynthetic pathway from gigantol to erianin, the possible substrates of the selected hydroxylases and OMTs were further analyzed using molecular docking. The three-dimensional protein model of hydroxylases and OMTs, which is positively correlated with the accumulation of erianin, was constructed using SWISS-MODEL and evaluated using UCLA-DOE LAB server v6.0 (Colovos and Yeates, 1993). Then, gigantol and compound 2 were docked into the active sites of OMTs as the substrate, while compound 1 was docked into that of hydroxylases. Most of the binding affinity predicted by AutoDock Vina were less than -5.0 kcal/mol, suggesting that they were relatively stable (Figure 7A). According to the standard of binding energy less than -6.0 kcal/mol, one tightly bound hydroxylase for compound 1 was screened out, while four OMTs were screened out in both gigantol and compound 2, respectively. These intermolecular interaction residues are listed in



Supplementary Table S5. For compound 1, gigantol, and compound 2, the conformation with the smallest binding energy is shown in Figure 7. Protein LOC110095638 had the best docking score on interaction with compound 1. Two hydrogen bonds (TRP 50 and HIS 35) and two Pi-Pi interactions (VAL 243 and AGR 245) were found between Protein LOC110095638 and compound 1 (Figure 7B). Conversely, four hydrogen bonds (VAL 121, VAL 128, GLY 123, and MET 125) were found between protein LOC110106749 and gigantol, which also resulted in stronger combination ability and lower affinity (Figure 7C). More Pi interaction, including Pi-Cation, Pi-Anion, Pi-Pi and Pi-Alkyl, were found between protein LOC110108303 and compound 2 (Figure 7D).

Overall, molecular docking results revealed the possible substrates of identified hydroxylases and OMTs and their catalytic mechanism. Moreover, potential key catalytic enzymes were further predicted in each step of the biosynthetic pathway from gigantol to erianin (Figure 8).

Conclusions

After a systematic analysis of benzyl compounds in DT and DC stems with significant differences in the content of erianin, gigantol was found to have similar structures with erianin and negatively correlated in content. Furthermore, deuterium-labeled gigantol was innovatively used to feed DC stems, and deuterium-labeled erianin was detected, suggesting gigantol might be one of the potential biosynthetic intermediates of erianin. To explore the biosynthetic pathway from gigantol to erianin in depth, comprehensive comparative metabolomic and transcriptomic analyses of DT and DC were conducted. The potential differentially expressed hydroxylases and OMTs that may play a key role in the pathway were screened out. The biosynthetic pathway from gigantol to erianin was proposed and the key enzymes during the biosynthesis steps were further predicted using molecular docking. This study not only clarified that gigantol was one of the biosynthetic intermediates of erianin, but also determined the biosynthetic pathway from gigantol to erianin, and identified hydroxylases and OMTs as the key modifying enzymes during the steps of this pathway. These findings would provide a clearer understanding of the biosynthetic pathway of erianin, and more attention should be devoted to the investigation on the biosynthetic pathway from 3,3'-trihydrobenzyl to gigantol and related enzymes.

Data availability statement

The datasets presented in this study can be found in online repositories. The names of the repository/repositories and accession number(s) can be found in the article/Supplementary Material.

References

Adejobi, O. I., Guan, J., Yang, L., Hu, J.-M., Yu, A., Muraguri, S., et al. (2021). Transcriptomic analyses shed light on critical genes associated with bibenzyl biosynthesis in *dendrobium officinale*. *Plants-Basel* 10 (4), 633. doi: 10.3390/plants10040633

Author contributions

LX: Conceptualization, Data curation, Funding acquisition, Investigation, Software, Visualization, Writing – original draft. QC: Investigation, Methodology, Visualization, Writing – review & editing. NC: Investigation, Methodology, Visualization, Writing – review & editing. YZ: Investigation, Methodology, Visualization, Writing – review & editing. YM: Conceptualization, Methodology, Supervision, Writing – review & editing. YTZ: Conceptualization, Resources, Writing – review & editing. KL: Conceptualization, Project administration, Resources, Writing – review & editing.

Funding

The author(s) declare financial support was received for the research, authorship, and/or publication of this article. This research was funded by the National Natural Science Foundation of China (Grant No. 32200215), the postdoctoral research grant in Henan Province (Grant No. 202103024), and the Henan Funiu Mountain Biological and Ecological Environment Observatory Research Project (HNFNBE20230105).

Conflict of interest

The authors declare that the research was conducted in the absence of any commercial or financial relationships that could be construed as a potential conflict of interest.

Publisher's note

All claims expressed in this article are solely those of the authors and do not necessarily represent those of their affiliated organizations, or those of the publisher, the editors and the reviewers. Any product that may be evaluated in this article, or claim that may be made by its manufacturer, is not guaranteed or endorsed by the publisher.

Supplementary material

The Supplementary Material for this article can be found online at: <https://www.frontiersin.org/articles/10.3389/fpls.2024.1436560/full#supplementary-material>

Akashi, T., Aoki, T., and Ayabe, S. (1998). CYP81E1, a cytochrome P450 cDNA of licorice (*Glycyrrhiza eChinata* L.), encodes isoflavone 2'-hydroxylase. *Biochem. Biophys. Res. Commun.* 251, 67–70. doi: 10.1006/bbrc.1998.9414

- An, T. N. M., Cuong, N. V., Quang, N. M., Thanh, T. V., and Alam, M. J. C. (2020). Green synthesis using PEG-400 catalyst, antimicrobial activities, cytotoxicity and in silico molecular docking of new carbazole based on α -aminophosphonate. *Chemistryselect* 5, 6339–6349. doi: 10.1002/slct.202000855
- Bari, M. S., Khandokar, L., Haque, E., Romano, B., Capasso, R., Seidel, V., et al. (2021). Ethnomedicinal uses, phytochemistry, and biological activities of plants of the genus *Gynura*. *J. Ethnopharmacology* 271. doi: 10.1016/j.jep.2021.113834
- Benkert, P., Tosatto, S. C. E., and Schomburg, D. (2008). QMEAN: A comprehensive scoring function for model quality assessment. *Proteins-Structure Funct. Bioinf.* 71, 261–277. doi: 10.1002/prot.21715
- Chassy, A. W., Adams, D. O., and Waterhouse, A. L. (2014). Tracing phenolic metabolism in *Vitis vinifera* berries with ^{13}C -phenylalanine: implication of an unidentified intermediate reservoir. *J. Agric. Food Chem.* 62, 2321–2326. doi: 10.1021/jf402229u
- Chen, M.-F., Liou, S.-S., Kao, S.-T., and Liu, I. M. (2019). Erianin protects against high glucose-induced oxidative injury in renal tubular epithelial cells. *Food Chem. Toxicol.* 126, 97–105. doi: 10.1016/j.fct.2019.02.021
- Chen, W., Gong, L., Guo, Z., Wang, W., Zhang, H., Liu, X., et al. (2013). A novel integrated method for large-scale detection, identification, and quantification of widely targeted metabolites: application in the study of rice metabolomics. *Mol. Plant* 6, 1769–1780. doi: 10.1093/mp/ss080
- Chen, Y., Wang, Y., Liang, C., Liu, L., Song, X., Zhao, Y., et al. (2022). Characterization of the key bibenzyl synthase in *dendrobium sinense*. *Int. J. Mol. Sci.* 23 (12). doi: 10.3390/ijms23126780
- Colovos, C., and Yeates, T. O. (1993). Verification of protein structures - patterns of nonbonded atomic interactions. *Protein Sci.* 2, 1511–1519. doi: 10.1002/pro.5560020916
- Cui, H., Jiang, X., Zhang, T., Wang, Z., Long, R., Yang, Q., et al. (2020). The research progress of plant cytochrome P450 family. *Chin. J. Grassland* 42, 173–180. doi: 10.16742/j.zgdxkb.20190182
- Do, C.-T., Pollet, B., Thevenin, J., Sibout, R., Denoue, D., Barriere, Y., et al. (2007). Both caffeoyl Coenzyme A 3-O-methyltransferase 1 and caffeic acid O-methyltransferase 1 are involved in redundant functions for lignin, flavonoids and sinapoyl malate biosynthesis in *Arabidopsis*. *Planta* 226, 1117–1129. doi: 10.1007/s00425-007-0558-3
- Duo, M., Xingyong, L., Jinliang, S., Tao, L., Yadong, G., and Hongcheng, L.-P. (2018). Simultaneous identification and evaluation of dendrobium by HPLC. *Asia-Pacific Traditional Med.* 14, 51–55.
- Inoue, K., Sewalt, V. J. H., Ballance, G. M., Ni, W. T., Stürzer, C., and Dixon, R. A. (1998). Developmental expression and substrate specificities of alfalfa caffeic acid 3-O-methyltransferase and caffeoyl coenzyme A 3-O-methyltransferase in relation to lignification. *Plant Physiol.* 117, 761–770. doi: 10.1104/pp.117.3.761
- Lam, K. C., Ibrahim, R. K., Behdad, B., and Dayanandan, S. (2007). Structure, function, and evolution of plant O-methyltransferases. *Genome* 50, 1001–1013. doi: 10.1139/G07-077
- Li, Y., Chen, Q., Xie, X., Cai, Y., Li, J., Feng, Y., et al. (2020). Integrated metabolomics and transcriptomics analyses reveal the molecular mechanisms underlying the accumulation of anthocyanins and other flavonoids in cowpea pod (*Vigna unguiculata* L.). *J. Agric. Food Chem.* 68, 9260–9275. doi: 10.1021/acs.jafc.0c01851
- Liu, C. J., Huhman, D., Sumner, L. W., and Dixon, R. A. (2003). Regiospecific hydroxylation of isoflavones by cytochrome P450 81E enzymes from *Medicago truncatula*. *Plant J.* 36, 471–484. doi: 10.1046/j.1365-3113X.2003.01893.x
- Luo, Y., Chen, Y., Ji, X., Yan, S., Zhong, W., and Tian, M. (2019). RP-HPLC-UV determination of seven chemical constituents and principal component cluster analysis of *Dendrobium*. *Chin. Traditional Herbal Drugs* 50, 5336–5341.
- Mantovani, C., Prado, R. D. M., and Lopes Pivetta, K. F. (2018). Silicon foliar application on nutrition and growth of *Phalaenopsis* and *Dendrobium* orchids. *Scientia Hort.* 241, 83–92. doi: 10.1016/j.scienta.2018.06.088
- Marita, J. M., Ralph, J., Hatfield, R. D., Guo, D. J., Chen, F., and Dixon, R. A. (2003). Structural and compositional modifications in lignin of transgenic alfalfa down-regulated in caffeic acid 3-O-methyltransferase and caffeoyl coenzyme A 3-O-methyltransferase. *Phytochemistry* 62, 53–65. doi: 10.1016/S0031-9422(02)00434-X
- Morris, G. M., Huey, R., Lindstrom, W., Sanner, M. F., Belew, R. K., Goodsell, D. S., et al. (2009). AutoDock4 and AutoDockTools4: automated docking with selective receptor flexibility. *J. Comput. Chem.* 30, 2785–2791. doi: 10.1002/jcc.v30:16
- Narnoliya, L. K., Sangwan, N., Jadaun, J. S., Bansal, S., and Sangwan, R. S. (2021). Defining the role of a caffeic acid 3-O-methyltransferase from *Azadirachta indica* fruits in the biosynthesis of ferulic acid through heterologous over-expression in *Ocimum species* and *Withania somnifera*. *Planta* 253 (1). doi: 10.1007/s00425-020-03514-y
- Noel, J. P., Dixon, R. A., Pichersky, E., Zubieta, C., and Ferrer, J.-L. (2003). “Chapter two Structural, functional, and evolutionary basis for methylation of plant small molecules,” in *Recent Advances in Phytochemistry*. Ed. J. T. Romeo (Elsevier) 37, 37–58.
- Overkamp, S., Hein, F., and Barz, W. (2000). Cloning and characterization of eight cytochrome P450 cDNAs from chickpea (*Cicer arietinum* L.) cell suspension cultures. *Plant Sci.* 155, 101–108. doi: 10.1016/S0168-9452(00)00214-4
- Qiao, Q., Du, Y., and Xie, L. (2022). Research advances of erianin: Source, production, biological activities and pharmacological properties. *Pharmacol. Res. - Modern Chin. Med.* 2, 100059. doi: 10.1016/j.prmcm.2022.100059
- Reinecke, T., and Kindl, H. (1994). Characterization of bibenzyl synthase catalyzing the biosynthesis of phytoalexins of orchids. *Phytochemistry* 35, 63–66. doi: 10.1016/S0031-9422(00)90510-7
- Schwender, J. (2008). Metabolic flux analysis as a tool in metabolic engineering of plants. *Curr. Opin. Biotechnol.* 19, 131–137. doi: 10.1016/j.copbio.2008.02.006
- Su, C., Zhang, P., Liu, J., and Cao, Y. (2017). Erianin inhibits indoleamine 2, 3-dioxygenase - induced tumor angiogenesis. *Biomedicine Pharmacotherapy* 88, 521–528. doi: 10.1016/j.biopha.2017.01.090
- Vavricka, C. J., Takahashi, S., Watanabe, N., Takenaka, M., Matsuda, M., Yoshida, T., et al. (2022). Machine learning discovery of missing links that mediate alternative branches to plant alkaloids. *Nat. Commun.* 13. doi: 10.1038/s41467-022-28883-8
- Werner, R. A., and Schmidt, H. L. (2002). The in vivo nitrogen isotope discrimination among organic plant compounds. *Phytochemistry* 61, 465–484. doi: 10.1016/S0031-9422(02)00204-2
- Wiederstein, M., and Sippl, M. J. (2007). ProSA-web: interactive web service for the recognition of errors in three-dimensional structures of proteins. *Nucleic Acids Res.* 35, W407–W410. doi: 10.1093/nar/gkm290
- Xia, J., Yin, F., Fang, J., Lou, G., Yu, J., Xu, Z., et al. (2023). Comprehensive chemical profiling of two *Dendrobium* species and identification of anti-hepatoma active constituents from *Dendrobium chrysotoxum* by network pharmacology. *BMC Complementary Med. Therapies* 23. doi: 10.1186/s12906-023-04048-y
- Yang, Q., He, Y., Kabahuma, M., Chaya, T., Kelly, A., Borrego, E., et al. (2017). A gene encoding maize caffeoyl-CoA O-methyltransferase confers quantitative resistance to multiple pathogens. *Nat. Genet.* 49, 1364–1364+. doi: 10.1038/ng.3919
- Yang, Y., and Liu, F. (2014). Study of dendrobium from yunnan by fourier transform infrared spectroscopy combined with hierarchical cluster analysis. *Chin. J. Inf. Traditional Chin. Med.* 21, 75–89.
- Yuan, S., Chan, H. C. S., and Hu, Z. (2017). Using PyMOL as a platform for computational drug design. *Wiley Interdiscip. Reviews-Computational Mol. Sci.* 7 (2). doi: 10.1002/wcms.2017.7.issue-2
- Yuan, Z., Wu, Q., Deng, J., Luo, K., He, J., and Yin, L. (2018). The mechanism of erianin relieving peritonitis caused by *Staphylococcus aureus*. *J. Hunan Agric. University. Natural Sci.* 44, 553–558. doi: 10.13331/j.cnki.jhau.2018.05.018
- Zhang, G.-Q., Liu, K.-W., Li, Z., Lohaus, R., Hsiao, Y.-Y., Niu, S.-C., et al. (2020). The *Apostasia* genome and the evolution of orchids. *Nature* 583, E30–E30. doi: 10.1038/s41586-020-2524-1
- Zhang, H., Gao, S., Lercher, M. J., Hu, S., and Chen, W.-H. (2012). EvolView, an online tool for visualizing, annotating and managing phylogenetic trees. *Nucleic Acids Res.* 40, W569–W572. doi: 10.1093/nar/gks576
- Zhang, T., Ouyang, H., Mei, X., Lu, B., Yu, Z., Chen, K., et al. (2019a). Erianin alleviates diabetic retinopathy by reducing retinal inflammation initiated by microglial cells via inhibiting hyperglycemia-mediated ERK1/2-NF- κ B signaling pathway. *FASEB J.* 33, 11776–11790. doi: 10.1096/fj.201802614RRR
- Zhang, Y., Lv, H.-P., Ma, C.-Y., Guo, L., Tan, J.-F., Peng, Q.-H., et al. (2015). Cloning of a caffeoyl-coenzyme A O-methyltransferase from *Camellia sinensis* and analysis of its catalytic activity. *J. Zhejiang University-Science B* 16, 103–112. doi: 10.1631/jzus.B1400193
- Zhang, Y., Zhang, Q., Wei, F., and Liu, N. (2019b). Progressive study of effects of erianin on anticancer activity. *Oncotargets Ther.* 12, 5457–5465. doi: 10.2147/OTT.S200161
- Zhong, R. Q., Morrison, W. H., Himmelsbach, D. S., Poole, F. L., and Ye, Z. H. (2000). Essential role of caffeoyl coenzyme A O-methyltransferase in lignin biosynthesis in woody poplar plants. *Plant Physiol.* 124, 563–577. doi: 10.1104/pp.124.2.563
- Zhong, R. Q., Morrison, W. H., Negrel, J., and Ye, Z. H. (1998). Dual methylation pathways in lignin biosynthesis. *Plant Cell* 10, 2033–2045. doi: 10.1105/tpc.10.12.2033
- Zou, Y., Xiao, C.-F., Zhong, R.-Q., Wei, W., Huang, W.-M., and He, S.-J. (2008). Synthesis of combretastatin A-4 and erianin. *J. Chem. Res.* 2008 (6), 354–356. doi: 10.3184/030823408X324751